

# Intermolecular Interactions, Solute Descriptors, and Partition Properties of Neutral Per- and Polyfluoroalkyl Substances (PFAS)

Satoshi Endo\*



Cite This: *Environ. Sci. Technol.* 2023, 57, 17534–17541



Read Online

ACCESS |



Metrics & More



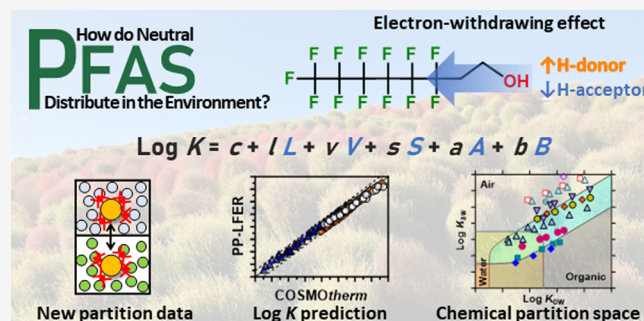
Article Recommendations



Supporting Information

**ABSTRACT:** The environmental partition properties of perfluoroalkyl and polyfluoroalkyl substances (PFAS) must be understood for their transport and fate analysis. In this study, isothermal gas chromatographic (GC) retention times of 60 neutral PFAS were measured using four columns with different stationary phase polarities, which indicated varying polar interactions exerted by these substances. The GC data were combined with new octanol/water partition coefficient data from this study and existing partition coefficient data from the literature and used to determine the polyparameter linear free energy relationship (PP-LFER) solute descriptors. A complete set of the solute descriptors was obtained for 47 PFAS, demonstrating the characteristic intermolecular interaction properties, such as hydrogen bonding capabilities influenced by the electron-withdrawing perfluoroalkyl group. The partition coefficients between octanol and water, air and water, and octanol and air predicted by the PP-LFER models agreed with those predicted by the quantum chemically based model COSMOtherm, suggesting that both models are highly accurate for neutral PFAS and can fill the current large data gaps in partition property data. A chemical partitioning space plot was generated by using the PP-LFER-predicted partition coefficients, showing the primary importance of the air phase for the environmental distribution of nonpolar and weakly polar PFAS and the increasing significance of organic phases with increasing PFAS polarity.

**KEYWORDS:** fluorotelomer substance, perfluoroalkane sulfonamide, gas chromatographic retention factor, linear solvation energy relationship, hydrogen bonding, chemical partitioning space



## INTRODUCTION

Per- and polyfluoroalkyl substances (PFAS) are of increasing concern due to their potential adverse effects on human health and ecosystems. Despite the high level of concern, the equilibrium partition properties of PFAS remain to be elucidated. Even basic property data such as octanol/water partition coefficients ( $K_{ow}$ ) are scarce for PFAS.<sup>1–3</sup> To the best of my knowledge, only one scientific paper<sup>4</sup> has reported measured  $K_{ow}$  values for neutral PFAS with perfluoroalkyl chain lengths of 4 or more. Similarly, reliable air/water partition coefficients ( $K_{aw}$ ) were available for only a few neutral PFAS with  $(\text{CF}_2)_{\geq 4}$  until our group recently reported experimental values for 21 PFAS.<sup>5</sup>

The equilibrium partition of organic compounds is determined by the intermolecular interactions with the surrounding phases, including polar (e.g., hydrogen (H)-bonding) and nonpolar (i.e., van der Waals) interactions. This study focuses on neutral compounds and neutral species of ionizable compounds, since the partitioning of ionized compounds is controlled by different mechanisms.<sup>6</sup> For neutral organic compounds, polyparameter linear free energy relationships (PP-LFERs) with Abraham's solute descriptors can quantify the energetic contributions of the relevant intermo-

lecular interactions and describe partition coefficients in general.<sup>7</sup> The PP-LFER equation most applicable to PFAS is<sup>8,9</sup>

$$\text{Log } K = c + sS + aA + bB + vV + lL \quad (1)$$

where  $K$  is the partition coefficient (also referred to as the partition constant or the partition ratio) between the two phases of interest. The uppercase letters on the right side of eq 1 are the solute descriptors:  $S$ , dipolarity/polarizability parameter;  $A$ , solute H-bond donor property;  $B$ , solute H-bond acceptor property;  $V$ , McGowan's molar volume; and  $L$ , the logarithmic hexadecane/air partition coefficient ( $K_{Hxd/air}$ ) at 25 °C. The lowercase letters are referred to as system parameters, are calibrated by least-squares multiple linear regression (MLR) with typically 50 or more calibration data, and reflect the complementary interaction properties of the two phases. The terms with  $S$ ,  $A$ , and  $B$  describe the polar interactions, while

**Received:** September 12, 2023

**Revised:** October 16, 2023

**Accepted:** October 17, 2023

**Published:** November 1, 2023



those with *V* and *L* describe the nonspecific cavity formation and nonpolar interactions.

The PP-LFERs can conveniently predict a variety of partition coefficients for a given compound. While solute descriptors are available for several thousand compounds,<sup>10</sup> they are rarely available for PFAS. In the past, Goss et al.<sup>11</sup> determined solute descriptors for four fluorotelomer alcohols (FTOHs) and four fluorotelomer olefins (FTOs). Later, Endo and Goss<sup>9</sup> recalibrated the solute descriptors for FTOHs, which were evaluated again by Abraham and Acree.<sup>12</sup> In addition, descriptors for very short PFAS ( $C_{\leq 3}$ , mostly refrigerants) have been reported,<sup>13,14</sup> and the ABSOLV database stored on the UFZ-LSER website<sup>10</sup> lists descriptor values for several per- and polyfluorinated alkanes and alcohols of unknown origin. Solute descriptors are unavailable for other PFAS, including those that have been frequently detected in the environment such as other fluorotelomer compounds and perfluoroalkanesulfonamides (PFASAs) with different substitution patterns.<sup>15–17</sup>

In a previous study, our group measured the values of  $K_{\text{Hxd/air}}$ , the decadic logarithm of which is *L* in eq 1, for 64 neutral PFAS to elucidate their nonpolar interaction properties.<sup>18</sup> The study showed that *L* can be explained by summing the contributions from the fluorinated and nonfluorinated parts of the molecule. For the polar interaction properties, however, such a simple additive principle may not work because the polar functional group can be significantly influenced by the strongly electron-withdrawing perfluoroalkyl group. In fact, previous studies have shown that *A* values for 4:2, 6:2, and 8:2 FTOHs are higher than those of nonfluorinated alkyl alcohols and that *B* has the opposite relationship.<sup>9,11,12</sup> Such effects should have a major impact on the partition properties of fluorinated organic compounds in general.

The purpose of this study was to characterize the interaction properties of neutral PFAS and enable the prediction of their partition coefficients by determining the PP-LFER solute descriptors. While the most recent definition of PFAS includes even compounds with only one perfluorinated C atom,<sup>19</sup> the focus of this study is on PFAS with  $(\text{CF}_2)_{\geq 4}$ , as only highly fluorinated PFAS show characteristic partition properties compared to non-PFAS.<sup>20</sup> Isothermal gas chromatography (GC) retention times were measured on capillary columns of differing polarity. GC retention data are useful because they are relatively easy and fast to measure and are equivalent to partition coefficients, reflecting the intermolecular interactions between the compound and stationary phase. The measured GC retention data were combined with new  $K_{\text{ow}}$  data from this study and existing partition coefficient data from the literature and used to calibrate the PFAS solute descriptors. The resulting descriptors were used to predict partition coefficients, which were compared to predictions by the quantum chemically based COSMOtherm model for validation. Finally, the PP-LFER-predicted partition coefficients were used to create a chemical partitioning space plot to graphically compare the environmental partition characteristics of various PFAS and non-PFAS.

## MATERIALS AND METHODS

**Chemicals.** Sixty PFAS used in this study are listed in Table 1. Table S1 in the Supporting Information includes the providers, purities, and CAS registry numbers. Of these 60, 59 were used in our previous study<sup>18</sup> and 10:2 FTO was added to the current list. In addition, 78 nonfluorinated reference compounds with known solute descriptors were analyzed for

Table 1. List of PFAS Used in This Study

Name	Abbreviation	Group	Generic structure
1H,1H-Perfluorobutan-1-ol	3:1 FTOH	Fluorotelomer alcohols (FTOHs)	$\text{F}(\text{CF}_2)_n-(\text{CH}_2)_m-\text{OH}$
4,4,5,5,6,6,6-Heptafluorohexan-1-ol	3:3 FTOH		
1H,1H,2H,2H-Perfluorohexan-1-ol	4:2 FTOH		
5,5,6,6,7,7,8,8,8-Nonafluorooctan-1-ol	4:4 FTOH		
1H,1H,2H,2H-Perfluorooctan-1-ol	6:2 FTOH		
1H,1H-Perfluorooctan-1-ol	7:1 FTOH		
1H,1H,2H,2H-Perfluorodecan-1-ol	8:2 FTOH		
1H,1H,2H,2H-Perfluorododecan-1-ol	10:2 FTOH		
1H,1H,2H,2H-Perfluorotetradecan-1-ol	12:2 FTOH		
1H,1H,1H,2H-Perfluoroheptan-2-ol	5:2s FTOH		
N-Ethylperfluorohexanesulfonamidoethanol	EtFhSE	N-Alkylperfluoroalkanesulfonamidoethanols (FASes)	$\text{F}(\text{CF}_2)_n-\text{SO}_2-\text{N}(\text{CH}_2)_2-\text{OH}$
N-Ethylperfluorooctanesulfonamidoethanol	EtFOSE		
N-Methylperfluorooctanesulfonamidoethanol	MeFhSE		
N-Methylperfluorooctanesulfonamidoethanol	MeFOSE		
Perfluorobutanesulfonamide	PFBSA	Perfluoroalkanesulfonamides (PFASAs)	$\text{F}(\text{CF}_2)_n-\text{SO}_2-\text{NH}_2$
Perfluorohexanesulfonamide	PFHSA		
Perfluorooctanesulfonamide	PFOSA		
N-Methylperfluorobutanesulfonamide	MeFBSA	N-Alkylperfluoroalkanesulfonamides (FASAs)	$\text{F}(\text{CF}_2)_n-\text{SO}_2-\text{NH}-\text{CH}_3$
N-Methylperfluorohexanesulfonamide	MeFhSA		
N-Methylperfluorooctanesulfonamide	MeFOSA		
N-Ethylperfluorohexanesulfonamide	EtFhSA		
N-Ethylperfluorooctanesulfonamide	EtFOSA	Perfluoroalkane iodides (PFAIs)	$\text{F}(\text{CF}_2)_n-\text{I}$
Perfluorobutanesulfonyl fluoride	PFBSF		
Perfluorobutyl iodide	PFBI		
Perfluorohexyl iodide	PFHxI		
Perfluoroheptyl iodide	PFHpI		
Perfluorooctyl iodide	PFOnI		
Perfluorodecyl iodide	PFDI	Fluorotelomer iodides (FTIs)	$\text{F}(\text{CF}_2)_n-(\text{CH}_2)_m-\text{I}$
1H,1H,2H,2H-Perfluorohexyl iodide	4:2 FTI		
1H,1H-Perfluoroheptyl iodide	6:1 FTI		
1H,1H,7H-Perfluoroheptyl iodide	6:1 FTI-7H		
1H,1H,2H,2H-Perfluorooctyl iodide	6:2 FTI		
1H,1H,2H,2H-Perfluorodecyl iodide	8:2 FTI		
1,1,1,2,2,3,3-Heptafluoro-3-[(1,1,1,2,2,3,3-hexafluoro-3-[(1,1,1,2,2,3,3-hexafluoro-3-[(1,1,1,2,2,3,3-tetrafluoroethoxy)-2-propenyl]oxy)-2-propenyl]oxy]propane	FE-E3	Fluoroethers (FEs)	$\text{F}_7\text{C}_3\text{O}-[\text{CF}_2-\text{CF}_2-\text{O}]_n-\text{CHF}-\text{CF}_3$
1,1,1,2,4,4,5,7,7,8,10,10,11,13,13,14,14,15,15,15-Eicosafluoro-5,8,11-tris(trifluoromethyl)-3,6,9,12-tetraoxapentadecane	FE-E4		
1,1,1,2,4,4,5,7,7,8,10,10,11,13,13,14,16,16,17,17,18,18-Tricosafluoro-5,8,11,14-tetrakis(trifluoromethyl)-3,6,9,12,15-pentaaoxtadecane	FE-E5		
Allyl 1H,1H-perfluorooctyl ether	AFOE	-	-
1-(Heptafluoropropoxy)-1,2,2,2-tetrafluoro-1-iodoethane	FE-E1-I	-	-
Allyl perfluoroisopropyl ether	APIPE	-	-
Perfluorotripropyl amine	PFTPrA	Perfluoroalkyl amines (PFTAAs)	$\text{F}(\text{CF}_2)_n-\text{N}(\text{CF}_2)_2\text{F}$
Perfluorotributyl amine	PFTBA		
Perfluorononane	PFN	Perfluoroalkanes (PFAs)	$\text{F}(\text{CF}_2)_n-\text{F}$
Perfluorododecane	PFDoD		
1H,8H-Perfluorooctane	1,8-DHPFO	-	-
1,8-Divinylperfluorooctane	1,8-DVPFO	-	-
4-(Perfluorooct-1-yl)styrene	PFOSt	-	-
1H,1H,2H-Perfluoro-1-hexene	4:2 FTO	Fluorotelomer olefins (FTOs)	$\text{F}(\text{CF}_2)_n-\text{CH=CH}_2$
1H,1H,2H-Perfluoro-1-octene	6:2 FTO		
1H,1H,2H-Perfluoro-1-decene	8:2 FTO		
1H,1H,2H-Perfluoro-1-dodecene	10:2 FTO		
1H,1H,2H,2H-Perfluorooctyl acrylate	6:2 FTAC	Fluorotelomer acrylates (FTACs)	$\text{F}(\text{CF}_2)_n-\text{CH}_2-\text{CH}(\text{CO}_2\text{R})=\text{CH}_2$
1H,1H,2H,2H-Perfluorodecyl acrylate	8:2 FTAC		
1H,1H,2H,2H-Perfluorododecyl acrylate	10:2 FTAC		
1H,1H,2H,2H-Perfluorohexyl methacrylate	4:2 FTMAC	Fluorotelomer methacrylates (FTMACs)	$\text{F}(\text{CF}_2)_n-\text{CH}_2-\text{CH}(\text{CO}_2\text{R})=\text{CH}_2$
1H,1H,2H,2H-Perfluorooctyl methacrylate	6:2 FTMAC		
1H,1H,2H,2H-Perfluorodecyl methacrylate	8:2 FTMAC		
1H,1H,2H,2H-Perfluorododecyl methacrylate	10:2 FTMAC		
4-(1H,1H,2H-Perfluorooctyl)benzyl alcohol	6:2 FTBnOH	-	-
1H,1H,2H,2H-Perfluorodecyl acetate	8:2 FTAc	-	-

GC retention times. A complete list of these compounds with suppliers, purities, and CAS Registry numbers is provided in Table S2. GC grade acetone and *n*-hexane and LC/MS grade methanol from Fujifilm Wako Pure Chemical Corporation (Osaka, Japan) and *n*-octan-1-ol (>99.5%) from Tokyo Chemical Industry (Tokyo, Japan) were used as solvents. Tap water was treated by reverse osmosis and further purified with an Ultrapure Water System (RFU665DA, Advantec, Tokyo, Japan).

**Isothermal GC Retention Time Measurement.** The GC columns used were, from low to high polarity, HP-5ms Ultra Inert (poly[5% phenyl/95% methyl]siloxane equivalent; Agilent Technologies, Santa Clara, CA), DB-200 (poly[35% trifluoropropyl/65% methyl]siloxane; Agilent Technologies), DB-225ms (poly[50% cyanopropylphenyl/50% methyl]siloxane equivalent; Agilent Technologies), and SolGel-WAX (polyethylene glycol; Trajan, Ringwood, Australia). Column dimensions were all 30 m × 0.25 mm i.d. with a coating thickness of 0.25 μm.

The method for GC retention time measurements follows that of a previous study.<sup>18</sup> Briefly, a 7890A/5975C GC/MS instrument (Agilent Technologies) equipped with an MPS2 autosampler and CIS4 injector (Gerstel, Mülheim an der Ruhr, Germany) was used for all measurements. For each column, isothermal retention times were measured at four temperatures in the range of 30–120 °C to cover all target compounds. The temperature at the injector and transfer line was fixed at 120 °C. The carrier gas was He at a flow rate of 1.2 mL/min. Compounds were introduced into the GC by injecting either headspace (100–250 μL) above the pure compound or solution in acetone (1 μL). Split injections were performed with a split ratio of 20–250. Column dead time ( $t_0$ ) was determined by injecting air and measuring Ar ( $m/z$  40). From the measured retention time ( $t$ ), the retention factor ( $k$ ) was calculated as  $k = (t - t_0)/t_0$ . Measurements with  $t < t_0 + 0.1$  min were considered too short and discarded. For each column and temperature,  $k$  values were obtained for 29–52 PFAS and 29–48 reference compounds. Only one injection was performed for each compound because repeated measurements showed that the  $k$  variation was typically within 0.01 log unit. Because multiple isomer peaks were observed in the chromatograms for fluoroether (FE)-F4 and FE-F5, the log  $k'$  value corresponding to the middle peak was used to represent all isomers, as previously done.<sup>18</sup>

**$K_{ow}$  Measurement.**  $K_{ow}$  was measured for nine PFAS (Table 2) to supplement the data set for descriptor determination. The nine PFAS were selected based on measurement feasibility and structural diversity. The shared-headspace or batch partition method was used as described previously.<sup>5</sup> Details of the methods are given in SI-1.

**Solute Descriptor Determination.** The standard procedure for solute descriptor determination was as follows. First, the system parameters in eq 1 were calibrated for each column (or partition system) and temperature by MLR using log  $k$  (or log  $K$ ) data and solute descriptors for reference compounds. Solute descriptor values for the reference compounds are listed in Table S3. Dimethylformamide, 1-pentylamine, dimethylsulfoxide, and dodecamethylcyclotetrasiloxane (D6) were removed from the log  $k$  data sets, because they frequently appeared as outliers (>3 SD) of the PP-LFER model fit. Reference data sets for hexadecane/water partition coefficients ( $K_{Hxd/w}$ ),<sup>21</sup>  $K_{ow}$ ,<sup>22</sup> and octanol/air partition coefficients ( $K_{oa}$ )<sup>23</sup> were taken from the cited references and amended with data for organosilicon compounds.<sup>24,25</sup> Similar to PFAS, organosilicon compounds

**Table 2. Measured Log  $K_{ow}$  Values at 25 °C for Neutral PFAS**

	Mean ± SD	Method
3:3 FTOH	2.46 ± 0.00	SH
4:4 FTOH	3.54 ± 0.00	SH
7:1 FTOH	5.01 ± 0.02	SH
5:2s FTOH	3.80 ± 0.03	SH
6:1 FTI	5.57 ± 0.01	SH
6:1 FTI-7H	4.90 ± 0.01	SH
PFBSA	2.85 ± 0.02	BP
MeFBSA	3.51 ± 0.00	BP
MeFBSE	3.11 ± 0.04	BP
4:2 FTOH <sup>a</sup>	3.30 ± 0.04	BP
6:2 FTOH <sup>a</sup>	4.54 ± 0.01	BP
8:2 FTOH <sup>a</sup>	5.58 ± 0.06	BP

<sup>a</sup>Data are from ref 4. SH, shared-headspace method; BP, batch partition method.

have weak van der Waals interaction properties<sup>9</sup> and it may be beneficial to include them in reference data sets. The solute descriptors for PFAS were then back-calculated by using the calibrated PP-LFER equations. Of the five descriptors,  $V$  can be calculated from the molecular structure<sup>26</sup> (note: the fragment value for F from Goss et al.<sup>11</sup> was used), and  $L$  was available for the PFAS studied.<sup>18</sup> Thus, the left side of eq 2 was known, and MLR was performed to obtain  $S$ ,  $A$ , and  $B$  on the right side.

$$\log K(\text{or } \log k) - c - \nu V - lL = sS + aA + bB \quad (2)$$

To determine the three descriptors, a minimum of three  $k$  and  $K$  data are required for a given PFAS compound. The data used here were:  $k$  measured for 60 PFAS in this study,  $K_{Hxd/w}$  for 21 PFAS,<sup>5</sup>  $K_{ow}$  for 12 PFAS (see the Results and Discussion section), and  $K_{oa}$  for 3 PFAS.<sup>11</sup> Note that  $K_{aw}$  for 21 PFAS in ref 5 was not considered here to avoid duplicate data use, as these data were derived from  $K_{Hxd/w}$  and  $K_{Hxd/air}$  through the thermodynamic cycle calculation.

Key to the accurate determination of the polar interaction descriptors is the availability of  $K$  data for partition systems with water as a partition phase because water is a strong H-bond donor and acceptor phase and thus the corresponding  $K$  values are sensitive to the H-bonding properties of the solute.<sup>27</sup> In particular, at least one solvent/water or air/water partition coefficient is required to determine  $B$  because there is no commonly used GC phase that is a significant H-bond donor. In the data set,  $K_{Hxd/w}$  is sensitive to both  $A$  and  $B$  and  $K_{ow}$  is sensitive to  $B$ . However,  $K_{Hxd/w}$  and  $K_{ow}$  data are not available for all PFAS. To increase the number of PFAS for which descriptors can be determined, the following assumptions were made. First, PFAS that have the same nonfluorinated structure and differ only in the perfluoroalkyl chain length share the values of  $S$ ,  $A$ , and  $B$ . Examples of this case are 4:2, 6:2, 8:2, 10:2, and 12:2 FTOHs. Second,  $A$  and/or  $B$  were set to 0 if the compound did not have a functional group that can form an H-bond in the respective manner. For example,  $A$  and  $B$  were set to 0 for perfluoroalkanes (PFAs), perfluoroalkyl iodides (PFAIs), and FTOs;  $A$  was set to 0 for X:2 fluorotelomer iodides (FTIs), acrylates (FTACs), and methacrylates (FTMACs); and  $B$  was set to 0 for 1H,8H-perfluorooctane (1,8-DHPFO). All of these assumptions are tabulated in Table S4.

Initially, the PP-LFER system parameters were calibrated by using only the data for nonfluorinated reference compounds and used to determine the solute descriptors for PFAS, as described above. However, this straightforward approach resulted in



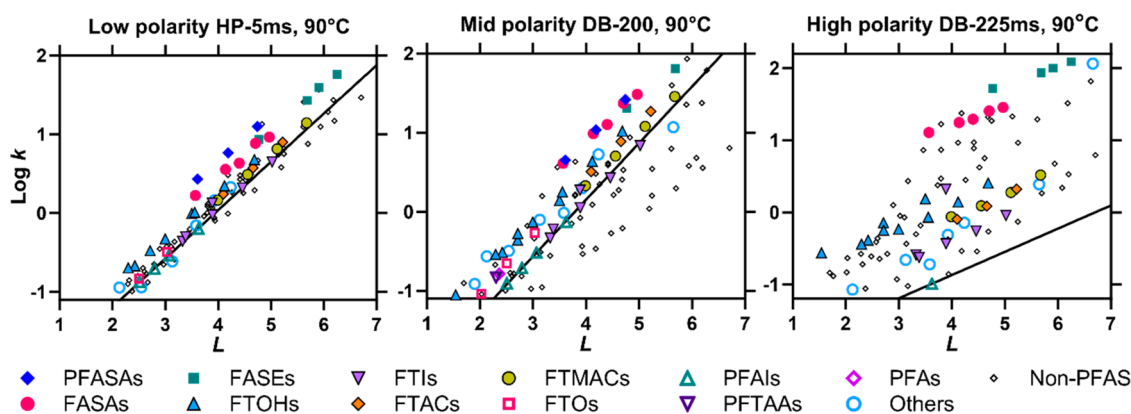


**Figure 1.** Examples of log GC retention factors ( $\log k$ ) against log hexadecane/air partition coefficients ( $L$ ). The lines indicate the nonpolar PFAS baselines generated with the mean of the slopes for PFAIs, FTOs, and FTIs and the intercept adjusted to the data for PFAIs. Data for other temperatures are shown in Figures S2–S5.

inconsistent descriptor values for some PFAS, as indicated by relatively large standard errors of descriptor values or unexpected negative  $A$  or  $B$  values. The reason for this is likely the problem of extrapolation; the system parameters calibrated with only nonfluorinated compounds are not applicable to PFAS.<sup>9,18</sup> To circumvent this problem, the system parameters of eq 1 and the solute descriptors for PFAS were determined iteratively in this work. The complete scheme of the iterative calculation is shown in Figure S1. In this iterative calculation, relatively data-rich PFAS (i.e., FTOHs, PFASAs,  $N$ -alkylperfluoroalkanesulfonamides (FASAs),  $N$ -alkylperfluoroalkanesulfonamidoethanols (FASEs), PFAIs, FTIs, FTOs, FTACs, and FTMACs; see Table S5) were included in the calibration sets and used to tentatively calibrate the system parameters. The  $S$ ,  $A$ , and  $B$  descriptor values predicted by the IFS-QSAR of EAS-E Suite<sup>28</sup> were used as initial values for PFAS. The obtained system parameters were then used to update the PFAS descriptors, and using these updated PFAS descriptors, the system parameters were recalibrated, and so on. This cycle was repeated 20 times, which was sufficient to obtain stable results.  $L$  was also updated from the reported values<sup>18</sup> in this iterative calculation using the literature data for nonpolar GC columns (squalane, SPB-Octyl,<sup>18</sup> and Apolane)<sup>11</sup> because small influences of polar interactions on  $\log k$ , which were not considered in the previous studies,<sup>11,18</sup> could be taken into account with the values of  $S$  and  $A$  for PFAS. The differences from the previous values, however, were small.

**Prediction by COSMOtherm.** The partition coefficients were predicted by the COSMOtherm algorithm, which follows the COSMO-RS theory<sup>29</sup> and can derive activity-related properties including partition coefficients, based on quantum chemical and statistical thermodynamic calculations. The programs Turbomole, COSMOConfX, and COSMOthermX (version 2021, COSMOlogic, Dassault Systèmes) were used for the calculation. More details about the method have been explained elsewhere.<sup>5,18</sup>

## RESULTS AND DISCUSSION

**Isothermal GC Retention Behavior of Neutral PFAS.** A total of 529 and 642  $\log k$  data were measured for PFAS and nonfluorinated reference compounds, respectively (Tables S6 and S7, Figure S2–S5). For each column and compound,  $\log k$  was linear against  $1/T$  (Figure S6), confirming the high measurement consistency over temperature.  $\log k$  data for a

given class of PFAS (e.g., X:2 FTOHs) for the HP-5ms and DB-200 columns were perfectly linear against the number of  $\text{CF}_2$  units (Figure S7). However, the relationship for DB-225ms was very slightly concave upward, and it was more so for SolGel-WAX. Since linearity is a prerequisite for PP-LFER model fitting, the  $\log k$  data for SolGel-WAX were not used for solute descriptor determination. For polar stationary phases, the contribution of interfacial adsorption to retention, in addition to the bulk partition mechanism, has been shown to be significant in some cases,<sup>30</sup> which may be a reason for the observed nonlinearity.

The  $\log k$  values for the low-polar HP-5ms column show a high correlation with  $L$  (Figure 1). Clearly, the nonpolar van der Waals interactions are prevalent with HP-5ms, and additional polar interactions have only minor influences on  $\log k$ . The correlation between  $\log k$  for the DB-200 column and  $L$  is less good, and a high scatter is evident for the highly polar DB-225ms and SolGel-Wax columns. For all columns,  $\log k$  for nonpolar PFAS (i.e., without a polar functional group, e.g., PFAs, PFAIs, and FTOs) shows a linear relationship with  $L$  and forms a baseline in the  $\log k$ – $L$  plot. Other PFAS deviate upward from the PFAS baseline, depending on their polarities. This is most evident in the DB-225ms and SolGel-WAX data; PFASAs and their  $N$ -substituted compounds are farthest from the nonpolar PFAS in the plot, reflecting their strong polarity, followed by the moderately polar FTOHs. The other fluorotelomer compounds (i.e., FTACs, FTMACs, and FTIs) deviate slightly from the baseline, reflecting their weak polarity. The GC retention measurement is therefore useful to roughly assess the polarity of PFAS. The relevant types of polar interactions are discussed quantitatively in the following section.

**$K_{ow}$  Measurement.** The measured  $K_{ow}$  values are presented in Table 2 along with the literature data for three FTOHs. This data set covers most of the target PFAS classes that are expected to have both  $A$  and  $B > 0$  and for which the availability of  $K$  data is particularly important for descriptor determination.

**Solute Descriptor Determination.** The final adjusted solute descriptors for all PFAS are presented in Table S8, and those for selected PFAS are shown in Table 3. Table S8 also shows the number of data available for each PFAS or PFAS group. The system parameters for all GC columns and partition systems are given in Table S9. All five solute descriptors are now available for 47 neutral PFAS. For the remaining 13 PFAS, the values of  $S$ ,  $A$ ,  $V$ , and  $L$  are available, but the value of  $B$  is missing due to a lack of  $K$  data. The quality of solute descriptor fitting

**Table 3. Solute Descriptor Values ( $\pm$ SE) for Selected PFAS Determined in This Study**

	S	A	B
X:1 FTOHs	0.30 $\pm$ 0.02	0.84 $\pm$ 0.02	0.14 $\pm$ 0.01
X:2 FTOHs	0.35 $\pm$ 0.02	0.60 $\pm$ 0.01	0.31 $\pm$ 0.01
5:2s FTOH	0.39 $\pm$ 0.02	0.62 $\pm$ 0.02	0.19 $\pm$ 0.01
PFASAs	0.96 $\pm$ 0.03	1.15 $\pm$ 0.03	0.23 $\pm$ 0.02
N-alkyl-FASAs	0.88 $\pm$ 0.02	0.74 $\pm$ 0.02	0.24 $\pm$ 0.01
N-alkyl-FASEs	1.00 $\pm$ 0.02	0.55 $\pm$ 0.03	0.68 $\pm$ 0.02
PFAIs	0.07 $\pm$ 0.01	0	0
X:2 FTIs	0.32 $\pm$ 0.01	0	0.17 $\pm$ 0.01
6:1 FTI	0.27 $\pm$ 0.02	0.13 $\pm$ 0.02	0.11 $\pm$ 0.01
6:1 FTI-7H	0.63 $\pm$ 0.04	0.24 $\pm$ 0.04	0.14 $\pm$ 0.02
PFAIs	−0.19 $\pm$ 0.06	0	0
X:2 FTOs	0.11 $\pm$ 0.01	0	0
X:2 FTACs	0.54 $\pm$ 0.01	0	0.40 $\pm$ 0.01
X:2 FTMACs	0.53 $\pm$ 0.01	0	0.39 $\pm$ 0.01

was high, with SDs generally  $<0.1$  log units. The relatively high SDs (0.1–0.5) were obtained only for PFAs, FEs, and perfluorotrialkylamines (PFTAAs), suggesting that the uncertainty of the descriptor values for these PFAS may be high. The reason for the low fit is currently unknown but could be related to the particularly high degree of fluorination of these PFAS, with little or no nonfluorinated substructure in the molecules.

**Solute Descriptor Values and Molecular Structure.** The *A* and *B* descriptors for FTOHs are higher and lower, respectively, than those for nonfluorinated alkan-1-ols (Figure 2), consistent with previous reports for X:2 FTOHs.<sup>9,11,12</sup> The secondary alcohol 5:2s FTOH also has high *A* and low *B* values. The increased H-bond acidity and decreased H-bond basicity of fluorinated alcohols such as 2,2,2-trifluoroethanol and 1,1,1,3,3,3-hexafluoropropan-2-ol have long been known<sup>31,32</sup> and can be explained by the electron-withdrawing effect of F on the  $-\text{OH}$  group. The results of this study demonstrate that this effect of F depends on the  $-\text{CH}_2-$  spacer length of FTOHs. Thus, 3:1 and 7:1 FTOHs (only one  $-\text{CH}_2-$  spacer) have the highest *A* and lowest *B* values of the FTOHs studied. As the spacer length increases, the influence of F on  $-\text{OH}$  diminishes and the *A* and *B* values approach those for nonfluorinated alcohols.

Not only FTOHs, but other PFAS also tend to have higher *A* values than their nonfluorinated counterparts, and the opposite is true for *B* values. For example, the *B* values of alkyl acrylates and methacrylates in the ABSOLV database are 0.42–0.55 and those of 1-iodoalkanes are 0.14–0.17.<sup>10</sup> These values are  $\sim 0.1$  lower than those of the corresponding fluorotelomer compounds. There are no descriptors for nonfluorinated alkane-sulfonamides, but the descriptors for nonfluorinated benzene-sulfonamides are available in the database. None of the variously substituted benzenesulfonamides have an *A* value greater than 1 or a *B* value less than 0.7, suggesting that the *A* (1.15) and *B* (0.26) values for PFASAs obtained in this work are significantly influenced by the perfluoroalkyl structure.

The descriptors of PFASAs, FASAs, and FASEs indicate that the *A* value decreases with the number of substitutions on the N atom (i.e.,  $-\text{SO}_2\text{NH}_2 > -\text{SO}_2\text{NHR} > -\text{SO}_2\text{N}(\text{C}_2\text{H}_5\text{OH})\text{R}$ ). The significant H-bond donor property of FASEs should be due to their hydroxyethyl group since the N atom does not have an H atom. The *B* values for PFASAs and FASAs are relatively low, and that of FASEs is higher due to the hydroxyethyl group.

In a previous article,<sup>5</sup> it was shown that 1H,1H,7H-perfluoroheptyl iodide (6:1 FTI-7H) has a relatively high affinity for water compared to 6:1 FTI. The electron-withdrawing F atoms were thought to make the H atom at the terminal methyl group of 6:1 FTI-7H significantly H-bond donating.<sup>5</sup> In fact, the *A* of 6:1 FTI-7H is positive (0.24) and higher than that of 6:1 FTI (0.13). However, incomplete fluorination affects not only *A* but also the *S* and *L* values. The *S* and *L* values of 6:1 FTI-7H are 0.63 and 3.89, respectively, and are higher than those of 6:1 FTI (0.27 and 3.38, respectively), although the size (*V*) of the two compounds is similar. A term-by-term analysis of the PP-LFER model indicates that the higher *S* of 6:1 FTI-7H than 6:1 FTI contributes more to the lower  $K_{\text{aw}}$  and  $K_{\text{Hxd/w}}$  values of 6:1 FTI-7H. Similarly, 1,8-DHPFO has *A*, *S*, and *L* values that are 0.24, 0.27, and 0.78 higher, respectively, than its perfluorinated counterpart, perfluorooctane. Increased *S* and *L* mean that partially hydrogenated PFAS interact more strongly with any phase than the fully fluorinated analogs do. Thus, even one or two H substitutions on the perfluoroalkyl chain make the molecule significantly more interactive, reducing the characteristically weak interaction properties of PFAS.

**Comparison to COSMOtherm Predictions.** Using the PP-LFER solute descriptors for PFAS and the system parameters

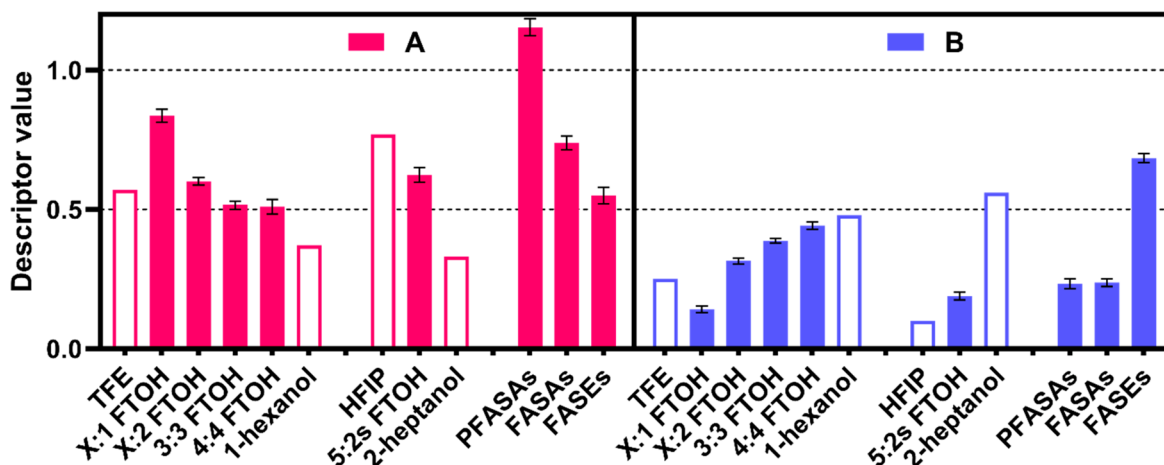


**Figure 2.** Solute H-bond donor (*A*) and acceptor (*B*) properties of selected PFAS. Solid bars are data from this study, and blank bars are data from the literature. Error bars indicate standard errors. 2,2,2-trifluoroethanol (TFE), 1,1,1,3,3,3-hexafluoro-2-propanol (HFIP).

obtained above, we calculated values for  $K_{ow}$ ,  $K_{aw}$ , and  $K_{oa}$  for the 47 neutral PFAS. Ideally, these predictions should be compared to external experimental data to validate the prediction accuracy. However, such data are not available. As an alternative approach, the predictions from the PP-LFERs were compared to those from COSMOtherm (Figure 3). The root mean squared errors

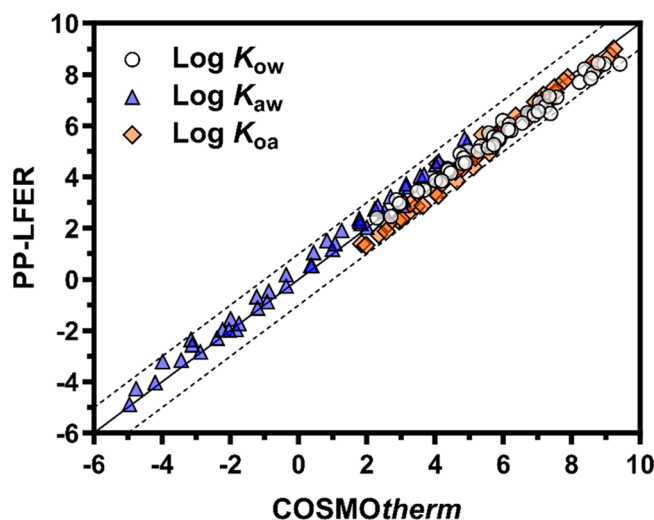


**Figure 3.** Partition coefficients predicted by PP-LFERs and COSMOtherm. The solid lines indicate the 1:1 agreement, and the dashed lines indicate the  $\pm 1$  log unit deviation.

(RMSE) for  $\log K_{ow}$ ,  $\log K_{aw}$ , and  $\log K_{oa}$  were 0.37, 0.42, and 0.33, respectively, indicating high agreement. Since the two prediction models are based on completely different principles, the agreement increases the reliability of both models. COSMOtherm provided, on average, 0.26 ( $\pm 0.27$ ) and 0.24 ( $\pm 0.23$ ) higher  $\log K_{ow}$  and  $\log K_{oa}$  predictions, respectively, and 0.33 ( $\pm 0.25$ ) lower  $\log K_{aw}$  values than the PP-LFERs. It is likely that the current version of COSMOtherm slightly overestimates the partitioning of PFAS from air to liquid phases, as reported in previous articles.<sup>5,18</sup> Note that some predictions from the PP-LFERs presented here cannot be considered “fully predicted” because the solute descriptors used were calibrated with the experimental data for  $K_{ow}$  and  $K_{aw}$ . Further comparison between PP-LFERs and COSMOtherm was performed for other solvent/water and solvent/air partition coefficients using the PP-LFER equations published in the literature<sup>8,33</sup> (Figure S8). Although the PP-LFER equations in the literature are often not calibrated with PFAS, the predictions of PP-LFERs and COSMOtherm agree within 1 log unit in most cases, similar to the results shown in Figure 3.

For comparison, the predictions from the EPI-Suite software provided by the U.S. EPA<sup>34</sup> were plotted against those from COSMOtherm (Figure S9). The RMSE values for  $\log K_{ow}$ ,  $\log K_{aw}$ , and  $\log K_{oa}$  were 0.27, 2.50, and 2.56, respectively, showing a large discrepancy for  $K_{aw}$  and  $K_{oa}$ . This result suggests that  $K_{aw}$  and  $K_{oa}$  predictions by EPI-Suite are inaccurate for many neutral PFAS.

**Chemical Partitioning Space Plot.** To provide an overview of the environmental phase partition properties of neutral PFAS, a chemical partitioning space plot was generated following the approach in the literature<sup>35,36</sup> (Figure 4). The figure plots  $\log K_{aw}$  against  $\log K_{ow}$ , both predicted by the PP-LFERs, and shows the equilibrium mass fractions of PFAS in a hypothetical system consisting of air, water, and an organic solid

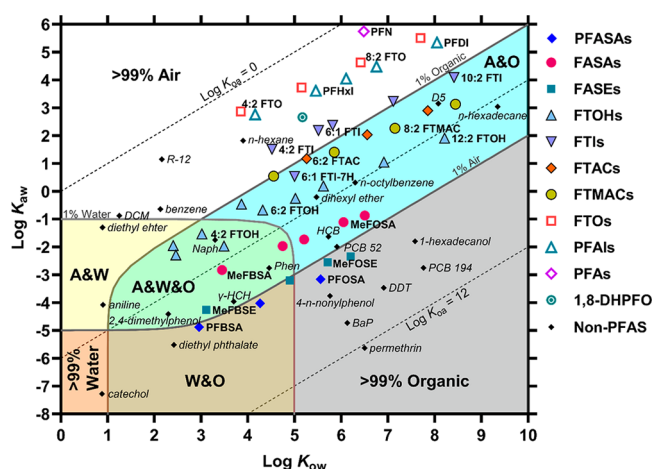


**Figure 4.** Chemical partitioning space plot for neutral PFAS. The volumes of air, water, and organic phase (represented by octanol) were  $10^6:10^3:1$ . Solid lines indicate 1% by mass of the chemicals in the respective phases. Dashed lines indicate  $\log K_{oa}$  values of 0, 6, and 12. Partition coefficients for PFAS were calculated by the PP-LFERs from this study, and those for the non-PFAS reference compounds were experimental values from the literature<sup>22,34,40–43</sup> or predicted by the PP-LFERs.<sup>10</sup> The acronyms indicate as follows: dichlorodifluoromethane (R-12), dichloromethane (DCM), decamethylcyclopentasiloxane (D5),  $\gamma$ -hexachlorocyclohexane ( $\gamma$ -HCH), naphthalene (Naph), phenanthrene (Phen), benzo[*a*]pyrene (BaP), hexachlorobenzene (HCB), polychlorinated biphenyl (PCB), and dichlorodiphenyltrichloroethane (DDT). Perfluorododecane is out of scale ( $\log K_{ow} = 8.4$ ,  $\log K_{aw} = 7.1$ ).

(represented by octanol). The volume ratios of these phases were assumed to be  $10^6:10^3:1$ , respectively, representing the environment as a whole.<sup>35,36</sup> Note that interfacial adsorption was not considered here for simplicity and the lack of parameters.

The 47 neutral PFAS are broadly distributed in the plot, reflecting the diversity of the properties. A general trend is that neutral PFAS prefer the air phase; the equilibrium mass in air is  $>99\%$  for 16 and at least 1% for 41 of the 47 compounds. In addition, water is often an unpreferred phase; the equilibrium mass in water is  $>1\%$  for only 10 PFAS. These features are well expected due to the weak van der Waals interactions with any phase and the high cavity energy in water of PFAS.

Looking at specific classes of PFAS, the nonpolar PFAS are all  $>99.9\%$  in the air phase, reflecting their extremely high volatility. Non-PFAS contaminants with similar phase distribution properties may be limited to alkanes and refrigerant compounds (e.g., R-12). Weakly polar PFAS (e.g., FTIs, FTACs) are primarily found in air, but with an appreciable organic phase contribution (0.1–20%). The more polar FTOHs are more abundant in the organic phase (2–70%). These distribution patterns of fluorotelomer compounds are comparable to those of medium to long alkyl compounds with no or a weakly polar functional group (e.g., *n*-hexadecane, dihexyl ether) and, notably, cyclic volatile methylsiloxanes (e.g., D5). PFASAs and their derivatives are even more in the organic phase, similar to moderately hydrophobic persistent organic pollutants (POPs), e.g., hexachlorocyclohexanes, hexachlorobenzene, and polychlorinated biphenyls with low degree of chlorination. Only short-chain PFAS with a polar functional group may be present in water at  $>1\%$ . Note that PFASAs and FASAs are weak acids and may ionize in water and partition more into water,<sup>5</sup> which is not accounted for in the plot. Figure S10 shows a plot for 134



neutral PFAS using the log  $K_{aw}$  and log  $K_{ow}$  values predicted by COSMOtherm. These neutral PFAS are from the lists of Kissel et al.<sup>37</sup> and our previous study.<sup>18</sup> The data points are even more widely distributed, although the plot again shows that air is the most important phase and that the air/organic phase distribution can be an important fate determinant, except for short-chain polar PFAS, which can also be in water.

An important question is the extent to which octanol can represent environmental organic phases for neutral PFAS. Available data for FTOHs suggest that soil organic carbon/water partition coefficients are  $\sim 2$  log units lower than  $K_{ow}$ .<sup>38</sup> If this is generally the case for neutral PFAS, then the organic phase contribution in Figure 4 is overestimated.

This study determined the PP-LFER solute descriptors of neutral PFAS that can be used to predict various partition coefficients. As noted above, many PP-LFER equations in the literature have not been calibrated with PFAS. Extrapolation may reduce prediction accuracy from what could otherwise be achieved.<sup>39</sup> This is not a problem specific to the PP-LFER models. Any empirical model requires high-quality data on PFAS to accurately predict PFAS properties, but such data are often lacking. In our series of studies, we measured  $K_{ow}$ ,  $K_{Hxd/w}$ , and  $K_{Hxd/air}$  for various neutral PFAS, which can also provide  $K_{aw}$  and  $K_{oa}$  values via thermodynamic cycles.  $K_{oa}$ ,  $K_{oil/w}$ , organic carbon/water, and liposome/water partition coefficients can be found in the literature for some FTOHs.<sup>9</sup> Measuring additional partition data for other PFAS or other partition systems would expand the applicability of the PP-LFER approach for PFAS. COSMOtherm is a theoretical model and may have the potential to provide accurate predictions without an additional empirical calibration. However, COSMOtherm is not free of charge and sometimes requires a long computation time for quantum chemical calculations, in contrast to the PP-LFER model. In the Supporting Information, COSMOtherm predictions for  $K_{ow}$ ,  $K_{aw}$ ,  $K_{oa}$ ,  $K_{Hxd/w}$ ,  $K_{Hxd/air}$  ( $L$ ),  $K_{Hxd/w}$ ,  $K_{oil/w}$ , and  $K_{oil/air}$  of 222 neutral (or neutral species of acidic) PFAS are provided for reference (Table S10). While reasonable accuracy (within  $\sim 1$  log unit) is expected, as discussed above, further validation of these predictions with experimental data is warranted.

## ■ ASSOCIATED CONTENT


### SI Supporting Information

The Supporting Information is available free of charge at <https://pubs.acs.org/doi/10.1021/acs.est.3c07503>.

Description of the measurement of  $K_{ow}$ ; tables listing the PFAS and reference compounds used, solute descriptors, measured log  $k$  values for PFAS, PP-LFER system parameters, and log  $K$  values predicted by COSMOtherm; and figures for schematic illustration of the iterative calculation procedure of descriptors and parameters, measured log  $k$  vs  $L$ , vs the number of  $CF_2$  units, and vs the reciprocal of temperature, predictions by PP-LFERs vs COSMOtherm for 47 PFAS, predictions by EPI-Suite and COSMOtherm, and a chemical partitioning space plot for 134 neutral PFAS (PDF)

## ■ AUTHOR INFORMATION

### Corresponding Author

Satoshi Endo – Health and Environmental Risk Division,  
National Institute for Environmental Studies (NIES),  
Tsukuba 305-8506 Ibaraki, Japan;  [orcid.org/0000-0001-](https://orcid.org/0000-0001-)

8702-1602; Phone: +81-29-850-2695;

Email: [endo.satoshi@nies.go.jp](mailto:endo.satoshi@nies.go.jp)

Complete contact information is available at:

<https://pubs.acs.org/doi/10.1021/acs.est.3c07503>

## Notes

The author declares no competing financial interest.

## ■ ACKNOWLEDGMENTS

I thank Yoko Katakura and Sadao Matsuzawa for their technical assistance. COSMOconfX and Turbomole were run on the NIES supercomputer system. This work was supported by the Environment Research and Technology Development Fund 3-2102 (JPMEERF20213002) of the Environmental Restoration and Conservation Agency provided by the Ministry of Environment of Japan.

## ■ REFERENCES

- (1) Wang, Z. Y.; MacLeod, M.; Cousins, I. T.; Scheringer, M.; Hungerbühler, K. Using COSMOtherm to predict physicochemical properties of poly- and perfluorinated alkyl substances (PFASs). *Environ. Chem.* **2011**, *8* (4), 389–398.
- (2) Ding, G.; Peijnenburg, W. J. G. M. Physicochemical properties and aquatic toxicity of poly- and perfluorinated compounds. *Crit. Rev. Environ. Sci. Technol.* **2013**, *43* (6), 598–678.
- (3) Lampic, A.; Parnis, J. M. Property estimation of per- and polyfluoroalkyl substances: A comparative assessment of estimation methods. *Environ. Toxicol. Chem.* **2020**, *39* (4), 775–786.
- (4) Carmosini, N.; Lee, L. S. Partitioning of fluorotelomer alcohols to octanol and different sources of dissolved organic carbon. *Environ. Sci. Technol.* **2008**, *42* (17), 6559–6565.
- (5) Endo, S.; Hammer, J.; Matsuzawa, S. Experimental determination of air/water partition coefficients for 21 per- and polyfluoroalkyl substances reveals variable performance of property prediction models. *Environ. Sci. Technol.* **2023**, *57* (22), 8406–8413.
- (6) Sigmund, G.; Arp, H. P. H.; Aumeier, B. M.; Bucheli, T. D.; Chefetz, B.; Chen, W.; Droge, S. T. J.; Endo, S.; Escher, B. I.; Hale, S. E.; Hofmann, T.; Pignatello, J.; Reemtsma, T.; Schmidt, T. C.; Schönsee, C. D.; Scheringer, M. Sorption and mobility of charged organic compounds: How to confront and overcome limitations in their assessment. *Environ. Sci. Technol.* **2022**, *56* (8), 4702–4710.
- (7) Abraham, M. H.; Ibrahim, A.; Zissimos, A. M. Determination of sets of solute descriptors from chromatographic measurements. *J. Chromatogr. A* **2004**, *1037* (1–2), 29–47.
- (8) Goss, K.-U. Predicting the equilibrium partitioning of organic compounds using just one linear solvation energy relationship (LSER). *Fluid Phase Equilib.* **2005**, *233* (1), 19–22.
- (9) Endo, S.; Goss, K.-U. Predicting partition coefficients of polyfluorinated and organosilicon compounds using polyparameter linear free energy relationships (PP-LFERs). *Environ. Sci. Technol.* **2014**, *48* (5), 2776–2784.
- (10) Ulrich, N.; Endo, S.; Brown, T. N.; Watanabe, N.; Bronner, G.; Abraham, M. H.; Goss, K. U., *UFZ-LSER database v 3.2*; <http://www.ufz.de/lserd> (accessed on 2023-06-30).
- (11) Goss, K.-U.; Bronner, G.; Harner, T.; Hertel, M.; Schmidt, T. C. The partition behavior of fluorotelomer alcohols and olefins. *Environ. Sci. Technol.* **2006**, *40*, 3572–3577.
- (12) Abraham, M. H.; Acree, W. E. Descriptors for fluorotelomere alcohols. Calculation of physicochemical properties. *Phys. Chem. Liquids* **2021**, *59* (6), 932–937.
- (13) Abraham, M. H.; Gil-Lostes, J.; Corr, S.; Acree, W. E., Jr. Determination of partition coefficients of refrigerants by gas liquid chromatographic headspace analysis. *J. Chromatogr. A* **2012**, *1265* (23), 144–148.
- (14) Abraham, M. H.; Gola, J. M. R.; Cometto-Muniz, J. E.; Cain, W. S. Solvation properties of refrigerants, and the estimation of their water-

solvent and gas-solvent partitions. *Fluid Phase Equilib.* **2001**, *180* (1–2), 41–58.

(15) Wang, Z.; Xie, Z.; Mi, W.; Möller, A.; Wolschke, H.; Ebinghaus, R. Neutral poly/per-fluoroalkyl substances in air from the Atlantic to the Southern Ocean and in Antarctic snow. *Environ. Sci. Technol.* **2015**, *49* (13), 7770–7775.

(16) Li, J.; Del Vento, S.; Schuster, J.; Zhang, G.; Chakraborty, P.; Kobara, Y.; Jones, K. C. Perfluorinated compounds in the Asian atmosphere. *Environ. Sci. Technol.* **2011**, *45* (17), 7241–7248.

(17) Ahrens, L.; Harner, T.; Shoeib, M.; Koblikova, M.; Reiner, E. J. Characterization of two passive air samplers for per- and polyfluoroalkyl substances. *Environ. Sci. Technol.* **2013**, *47* (24), 14024–14033.

(18) Hammer, J.; Endo, S. Volatility and nonspecific van der Waals interaction properties of per- and polyfluoroalkyl substances (PFAS): Evaluation using hexadecane/air partition coefficients. *Environ. Sci. Technol.* **2022**, *56* (22), 15737–15745.

(19) *Reconciling Terminology of the Universe of Per- and Polyfluoroalkyl Substances: Recommendations and Practical Guidance*; Series on Risk Management No. 61; Organisation for Economic Co-operation and Development, 2021.

(20) Goss, K.-U.; Bronner, G. What is so special about the sorption behavior of highly fluorinated compounds? *J. Phys. Chem. A* **2006**, *110* (30), 9518–9522.

(21) Abraham, M. H.; Whiting, G. S.; Fuchs, R.; Chambers, E. J. Thermodynamics of solute transfer from water to hexadecane. *J. Chem. Soc., Perkin Trans.* **1990**, *2* (2), 291–300.

(22) Abraham, M. H.; Chadha, H. S.; Whiting, G. S.; Mitchell, R. C. Hydrogen bonding. 32. An analysis of water-octanol and water-alkane partitioning and the  $\log p$  parameter of seiler. *J. Pharm. Sci.* **1994**, *83* (8), 1085–1100.

(23) Abraham, M. H.; Acree, W. E., Jr. Comparison of solubility of gases and vapours in wet and dry alcohols, especially octan-1-ol. *J. Phys. Org. Chem.* **2008**, *21* (10), 823–832.

(24) Xu, S.; Kropscott, B. Method for simultaneous determination of partition coefficients for cyclic volatile methylsiloxanes and dimethylsilanediol. *Anal. Chem.* **2012**, *84* (4), 1948–1955.

(25) Xu, S.; Kropscott, B. Octanol/air partition coefficients of volatile methylsiloxanes and their temperature dependence. *J. Chem. Eng. Data* **2013**, *58* (1), 136–142.

(26) Abraham, M. H.; McGowan, J. C. The use of characteristic volumes to measure cavity terms in reversed phase liquid chromatography. *Chromatographia* **1987**, *23* (4), 243–246.

(27) Endo, S.; Goss, K.-U. Applications of polyparameter linear free energy relationships in environmental chemistry. *Environ. Sci. Technol.* **2014**, *48* (21), 12477–12491.

(28) *EAS-E Suite* (Ver.0.95 - BETA, release Feb., 2022); ARC Arnot Research and Consulting Inc., Toronto, ON, Canada; [www.eas-e-suite.com](http://www.eas-e-suite.com).

(29) Klamt, A. Conductor-like screening model for real solvents: A new approach to the quantitative calculation of solvation phenomena. *J. Phys. Chem.* **1995**, *99* (7), 2224–2235.

(30) Poole, C. F.; Poole, S. K. Foundations of retention in partition chromatography. *J. Chromatogr. A* **2009**, *1216* (10), 1530–1550.

(31) Kamlet, M. J.; Abboud, J. L. M.; Abraham, M. H.; Taft, R. W. Linear solvation energy relationships. 23. A comprehensive collection of the solvatochromic parameters,  $\pi^*$ ,  $\alpha$ , and  $\beta$ , and some methods for simplifying the generalized solvatochromic equation. *J. Org. Chem.* **1983**, *48* (17), 2877–2887.

(32) Abraham, M. H. Scales of solute hydrogen-bonding: Their construction and application to physicochemical and biochemical processes. *Chem. Soc. Rev.* **1993**, *22* (2), 73–83.

(33) Flanagan, K. B.; Acree, W. E., Jr.; Abraham, M. H. Comments regarding "predicting the equilibrium partitioning of organic compounds using just one linear solvation energy relationship (LSER)". *Fluid Phase Equilib.* **2005**, *237* (1–2), 224–226.

(34) *EPI-Suite v4.11*; U.S. Environmental Protection Agency. <https://www.epa.gov/tsc-screening-tools/epi-suite-tm-estimation-program-interface> (last accessed 2023-09-12).

(35) Gama, S.; Arnot, J. A.; Mackay, D. Toxic organic chemicals. In *Encyclopedia of Sustainability Science and Technology*; Meyers, R. A., Ed.; Springer New York: New York, 2012; pp 10657–10671.

(36) Gouin, T.; Mackay, D.; Webster, E.; Wania, F. Screening chemicals for persistence in the environment. *Environ. Sci. Technol.* **2000**, *34* (5), 881–884.

(37) Kissel, J. C.; Titaley, I. A.; Muensterman, D. J.; Field, J. A. Evaluating neutral PFAS for potential dermal absorption from the gas phase. *Environ. Sci. Technol.* **2023**, *57* (12), 4951–4958.

(38) Liu, J.; Lee, L. S. Effect of fluorotelomer alcohol chain length on aqueous solubility and sorption by soils. *Environ. Sci. Technol.* **2007**, *41* (15), 5357–5362.

(39) Endo, S. Applicability domain of polyparameter linear free energy relationship models evaluated by leverage and prediction interval calculation. *Environ. Sci. Technol.* **2022**, *56* (9), 5572–5579.

(40) Wania, F.; Dugani, C. B. Assessing the long-range transport potential of polybrominated diphenyl ethers: A comparison of four multimedia models. *Environ. Toxicol. Chem.* **2003**, *22* (6), 1252–1261.

(41) Li, N.; Wania, F.; Lei, Y. D.; Daly, G. L. A comprehensive and critical compilation, evaluation, and selection of physical–chemical property data for selected polychlorinated biphenyls. *J. Phys. Chem. Ref. Data* **2003**, *32* (4), 1545–1590.

(42) Xiao, H.; Li, N.; Wania, F. Compilation, evaluation, and selection of physical-chemical property data for  $\alpha$ -,  $\beta$ -, and  $\gamma$ -hexachlorocyclohexane. *J. Chem. Eng. Data* **2004**, *49* (2), 173–185.

(43) Abraham, M. H.; Andonian-Haftvan, J.; Whiting, G. S.; Leo, A.; Taft, R. S. Hydrogen bonding. Part 34. The factors that influence the solubility of gases and vapors in water at 298 K, and a new method for its determination. *J. Chem. Soc., Perkin Trans.* **1994**, *2* (8), 1777–1791.